Solar Energy Materials & Solar Cells 96 (2012) 108–111

Contents lists available at SciVerse ScienceDirect

Solar Energy Materials & Solar Cells

journal homepage: www.elsevier.com/locate/solmat

Local investigation of thermal dependence of light emission from reverse-biased monocrystalline silicon solar cells

Lubomír Grmela [a], Pavel Škarvada [a], Pavel Tománek [a,*], Robert Macků [a], Steve Smith [b]

[a] Brno University of Technology, Faculty of Electrical Engineering and Communication, Department of Physics, Technická 8, 616 00 Brno, Czech Republic
[b] South Dakota School of Mines and Technology, Nanoscience and Nanoengineering, 501 E. St. Joseph Street, Rapid City, South Dakota 57701, USA

ARTICLE INFO

Article history:
Received 10 February 2011
Received in revised form
6 September 2011
Accepted 13 September 2011
Available online 1 October 2011

Keywords:
Silicon solar cell
Defect
Light emission
Reverse bias
Thermal characteristics
Localization

ABSTRACT

The quality and lifetime of solar cells critically depend on minimization of both bulk and surface imperfections. When a solar cell is reverse-biased with low voltage, weak emission from imperfections (pre-breakdown sites) appears. We report on the local measurement of such breakdown using a scanning near-field optical microscope. Due to the very weak signals, we use a cooled photomultiplier in the photon counting regime to achieve high sensitivity light detection. This technique allows non-destructive detection, localization and high spatial resolution of light-emitting centers originating from different imperfections in the cell. We have found that the emission from these pre-breakdown sites exhibits unique thermal characteristics. As a consequence, the thermal characteristics can distinguish among several kinds of imperfections in monocrystalline silicon solar cells.

1. Introduction

There is a wide variety of possible imperfections in devices with large area p-n junctions [1,2]. Some of them can be, in particular cases, harmless with respect to device performance, while others are not. Solar cells belong to a class of devices where the number of imperfections considerably affects their efficiency and lifetime [3,4]. For the detection and localization of such defects, different types of mapping and non-mapping techniques have been used [5–8]. With the development of charge coupled device (CCD) detectors, a number of fast imaging methods with applications to solar cell characterization have been found [9,10]. However, many questions relevant to the light emission from material defects in solar cells and their mechanisms still persist.

When a solar cell is reverse-biased, light emission in the visible spectrum occurs [11]. This emission has been generally attributed to local pre-breakdown or avalanche breakdown [12,13]. However, for small imperfections and low reverse bias voltage, the radiant flux of this emission is fairly weak. Therefore a combination of electrical measurement with high sensitivity, and scanning near-field optical microscopy (SNOM) in aperture and/or apertureless mode with sensitive detection, i.e. by photomultiplier tube (PMT), has been used in these investigations [7,8,14].

In this work, we present experimental results showing the different nature of select light-emitting centers (LECs) situated on the surface edges or inside the bulk of a reverse-biased solar cell. For this purpose we measured and compared the thermal characteristics of light emission vs. reverse bias voltage from select LECs on a monocrystalline silicon solar cell.

2. Experiment

Fig. 1 shows a scheme of our experimental setup.

A monocrystalline silicon solar cell wafer ($10 \times 10\ cm^2$), not yet installed in a solar panel, was used as the sample. The wafer was fabricated by standard diffusion technology but the anisotropic etching was skipped. Monocrystalline solar cells with pyramidal texturing exhibit too rough a surface for the microscopic SNOM studies, as the likelihood to damage the optical probe is high [5]. If the sample is made from truncated pyramidal structures, the use of SNOM is suitable, and our measurements of imperfections on anodic and acid etching texturization provide similar results [2].

A $10 \times 10\ cm^2$ cell was cut by diamond saw, mounted on a measuring electrode, reverse-bias loaded and thermally stabilized in a thermostat. Three temperatures (T=302 K, 314 K and 334 K) simulating cell operating temperatures have been selected, and thermal stabilization and electrical bias voltage were computer controlled.

* Corresponding autor. Tel.: +420 541 143 278; fax: +420 541 143 133.
E-mail address: tomanek@feec.vutbr.cz (P. Tománek).

0927-0248/$ - see front matter © 2011 Elsevier B.V. All rights reserved.
doi:10.1016/j.solmat.2011.09.029

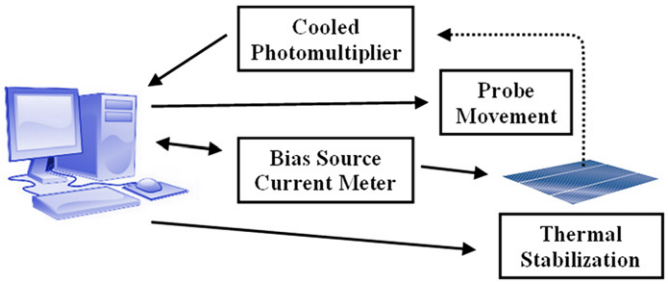

Fig. 1. Basic setup used for low light detection of thermally stabilized reverse-biased solar cell.

In our experiments a combination of two steps, reported by our colleagues in [6,15] were used: *I–U* measurements on the entire wafer in the reverse-bias voltage range show under which voltages a noise current from cell defects appears [6]. On the other hand, laser beam induced current (LBIC) is a method generally used for defect localization in structures of exposed p–n junctions [15]. Focused incident photons generate carriers in an optically excited p–n junction area. This local current response is then measured. When we insert an optical fiber probe, which scans over the sample surface, locally collected light emission is guided it to a PMT. A fast scan with a cleaved multimode fiber (aperture 50 μm) allows coarse localization of defect sites for these voltages.

Because a 10×10 cm^2 wafer is too large for the local measurement instrumentation, a corner with previously found imperfections was mechanically broken off into an approximately 15×15 mm^2. To avoid the probability of new contamination formed by the diamond saw mechanism in the vicinity of left and upper edges of the sample, the scanning area was further reduced to a 12×12 mm^2 zone containing a few of the original defects localized near the cell edge (LEC1) and in the bulk of the wafer (LEC2), respectively.

Local emission measurements with a cleaved single mode fiber (aperture 10 μm) were then taken to obtain better resolution. The highest resolution is obtained with a sharpened single mode fiber probe (aperture 60 nm) of SNOM [5,7], but it is a time consuming measurement. To obtain the highest sensitivity, a cooled PMT and single photon counting methods were used. Our PMT is mainly sensitive in the visible range (wavelength range from 350 nm to 800 nm).

3. Results and discussion

In the reverse-bias regime, we examined select imperfections on a 12×12 mm^2 surface at low reverse bias voltage, located near the edges and/or in the cell bulk. Light emission appeared over a wide voltage range (up to $U_r = -50$ V). In comparison with other techniques [10,16] we have observed the onset of light-emitting centers for threshold voltage as low as $U_r = -1.9$ V, at temperature $T = 302$ K, but the signal was too weak to be easily measured by generally used techniques. Fig. 2 shows the light emission vs. voltage characteristics of one of the low-voltage centers localized near the cell edge (LEC1). Repeated measurements obtained from 45 different LEC sites on the cell edges provided similar results. In CCD-based measurements, this minimum voltage value is slightly higher, due to the fact that the cooled PMT has a higher sensitivity. For accurate determination of the threshold voltage, for which light appears, a low noise system with high sensitivity is therefore needed. Such a system allows considerably improved sensitivity, however, spatially resolved measurements are time-consuming (*e.g.* a 30×30 pixel scan, with sensitivity 300 photons/s at 650 nm,

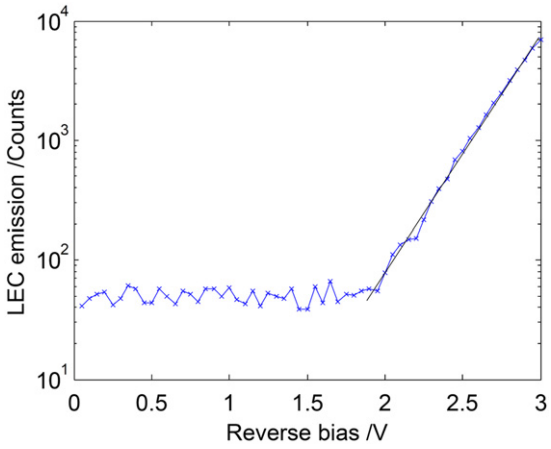

Fig. 2. Low reverse voltage light emission from LEC1, temperature $T = 302$ K, integration time $t = 0.2$ s.

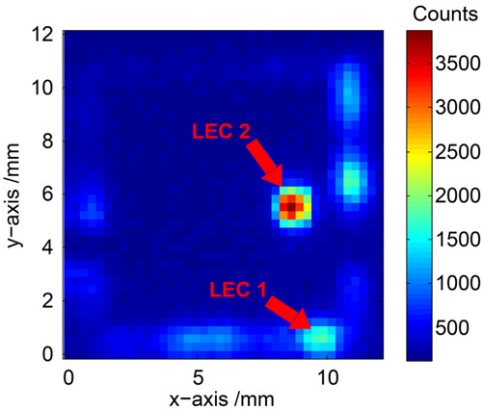

Fig. 3. Map of light emission in visible range from reverse-biased sample, $U_r = -12.8$ V, temperature $T = 302$ K. Here the left and upper edges of the sample are mechanically broken, while right and lower edges are the edges of original solar cell. The map was obtained with a single mode fiber probe, aperture 10 μm.

takes approximately 20 min). Values below 60 counts in Fig. 2 represent PMT dark counts.

Fig. 3 shows two principal kinds of LECs from the 12×12 mm^2 corner area of the sample. The map was obtained by scanning the sample with the single mode fiber probe (diameter of 10 μm), as discussed above. Two defects of a very different nature were revealed: LEC 1 located near the edge of original solar cell (approximately 40 μm), and LEC 2 located at a defect inside the cell (here 3 mm from the edge). Each of these imperfections emit light when the solar cell is reverse-biased enough (at least $U_r = -2$ V) (Fig. 2). Other very low light emissions from bulk defects similar to LEC 2 can also be observed over the whole sample (see Fig. 3). The resolution in this figure is about 1 mm because the scanning probe was used in constant height mode, and was quite far from the cell, due to its rough surface.

Nice results of light emission with high spatial resolution were obtained by Schneemann et al. [17]. Therefore to provide higher resolution measurements, it is necessary to cut smaller samples (here 12×12 mm^2 area) out of the larger wafer in order to mount them onto the piezotube sample stage. Fig. 4 represents an SNOM image (100×100 μm^2)of cell topography combined with a color map of the neighborhood of LEC1 site. It is interesting to remark, that defects often have larger dimensions than their corresponding LECs, and may also be formed by aggregation of small light emitting spots, as we reported previously [5].

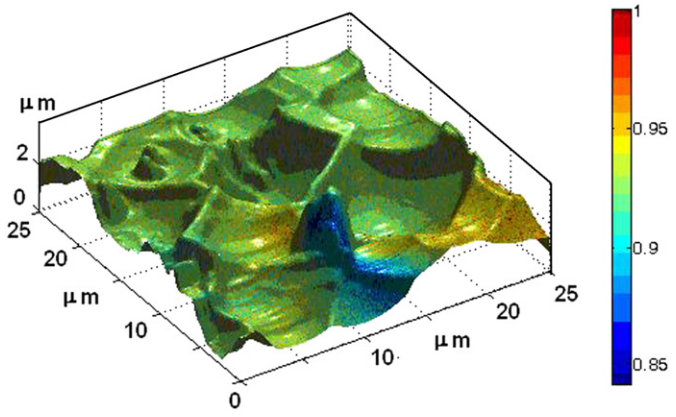

Fig. 4. SNOM image of solar cell sample (100×100) μm^2 showing a light emission from LEC1 near the original cell edge mapped on topography of the local structure of monocrystalline silicon truncated surface (blue peak): scanning velocity 18.5 μm/s, set point 8.9 V, feedback gain 0.5, $U_t = -12.8$ V. (For interpretation of the references to colour in this figure legend, the reader is referred to the web version of this article.)

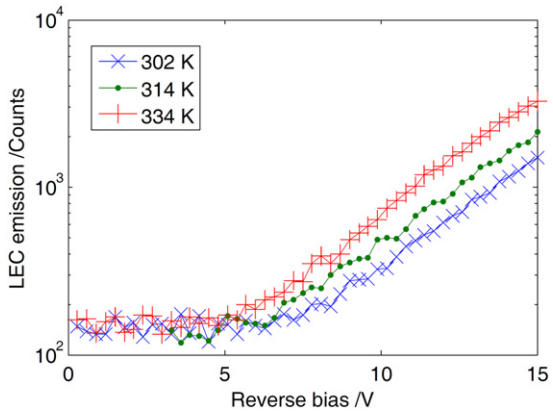

Fig. 5. Thermal dependence of light emission from edge defect LEC 1 (Fig.3) in reverse-biased sample cells.

Figs. 5 and 6 show light emission-voltage characteristics obtained with a cleaved single mode fiber probe placed over the defects for various sample temperatures. They allow a comparison of the thermal dependence of LEC 1 and LEC 2 on reverse-biased voltage. Three temperatures ($T = 302$ K, 314 K and 334 K) corresponding to normal cell temperatures if the cell is exposed to the sunlight, were chosen. Fig. 5 shows that light emission is thermally dependent for LEC 1, while Fig. 6 shows that light emission is almost thermally independent for LEC 2. The second important difference is that light emission increases more rapidly with voltage for LEC 2 at low reverse-biased voltages (-5 to -10 V).

As a complement to the previous optical measurements, *I–U* measurements in reverse-bias regime were also performed. Fig. 7 shows one partial breakdown in the sample with a negative thermal coefficient of the breakdown voltage. This result implies that for low reverse voltage the breakdown does not exhibit an avalanche behavior. In this case, breakdown voltages are similar to the threshold voltages for light emission in LEC 1, and also have similar thermal dependence.

Measured light emission from spot LEC1 reflects a positive thermal dependence, while a very weak negative thermal dependence from bulk spot LEC2 has been observed (Fig. 8). Thus this method allows us to identify defects in the cell and distinguish among different types of observed LECs.

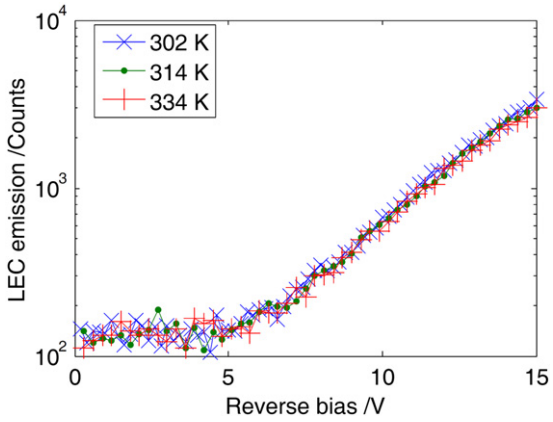

Fig. 6. Thermal dependence of light emission from bulk structure defect LEC 2 (Fig. 3) in reverse-biased sample.

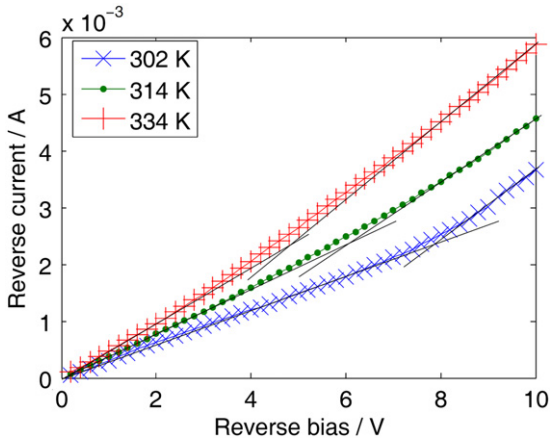

Fig. 7. Thermal dependence of reverse *I–U* characteristics.

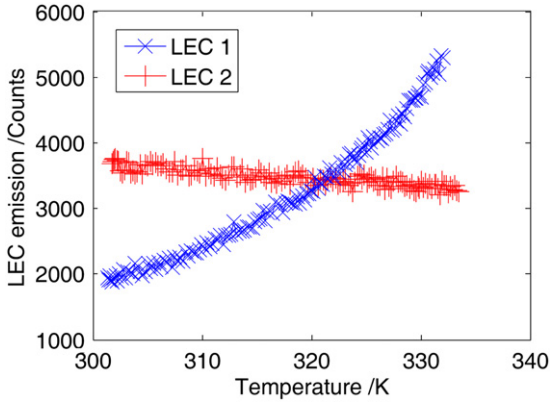

Fig. 8. Two spots visible light emission thermal dependence at $U_t = 12.8$ V.

4. Conclusion

The demonstrated method combines advantages of both separate electrical and local optical measurements, and offers non-destructive investigation with better localization of defects or inhomogeneities.

The novelty of this approach lies in the fact that by using local measurement with LBIC and SNOM with high sensitivity detection, we are able to obtain higher spatial resolution of very weak signals from inhomogeneities that are affecting the lifetime, quality and reliability of solar cells.

The resulting mapping technique used in this paper allows localization and distinguishing among select light-emitting centers (LECs) originating from various visible and hidden inhomogeneities in solar cells. It has been demonstrated that light emission from reverse biased solar cells can reveal structural inhomogenities. At least two distinct breakdown types from various inhomogeneity sites on the edges and interior regions of solar cells were thus distinguished (Fig. 8). The LECs from defects (inclusions) in bulk structure show weakly negative light emission temperature dependence, while the edge emission shows positive light emission temperature dependence.

While breakdown in bulk has the correct thermal dependence, the measured breakdown voltage in edge defect is probably not in the Zener or Schottky range. Considering the similarity of breakdown voltages and the threshold voltages for the LECs near the edge of the cell, the electrically measured imperfections could be caused by mechanical processing of solar cell edges. This edge isolation could also introduce a thermal breakdown.

In conclusion we can say that this method, together with a control of sample temperature, provides a basic classification of defects, similar to method of Wagner et al. [18]. We discovered, that only 30 K temperature range is sufficient for this classification. However, to precisely determine the nature of breakdowns near the edge of the studied cell, further local experiments with thermally a modified SNOM will be required.

Acknowledgment

This work has been supported by the Czech Ministry of Education in the frame of MSM 0021630503 Research Intention MIKROSYN "New Trends in Microelectronic System and Nanotechnologies", by GACR Grant P102/10/2013 "Fluctuation process in PN junctions of solar cells", and by Czech Ministry of Education Grant LH11060 "Study of local electric and optical characteristics of solar cells". Smith acknowledges funding provided by NASA award #NNX09AP67A, NSF award no.'s 0619890 (DMR), 0903804 (EPSCoR) and the State of South Dakota.

References

[1] D.K. Schroder, Semiconductor Material and Device Characterization, 3rd edn., Wiley-IEEE Press, Hoboken, New Jersey, 2006, pp. 82–96.

[2] P. Tománek, P. Škarvada, R. Macků, L. Grmela, Detection and localization of defects in monocrystalline silicon solar cell, Advances in Optical Technologies (2010) 1–5. doi:10.1155/2010/805325.

[3] S. Rein, Lifetime spectroscopy: a method of defect characterization in silicon for photovoltaic applications, Springer Series in Materials Science, Vol. 85, Springer, Heidelberg, 2005, pp. 25–32.

[4] M. Kasemann, W. Kwapil, B. Walter, J. Giesecke, B. Michl, M. The, J.-M. Wagner, J. Bauer, A. Schütt, J. Carstensen, S. Kluska, F. Granek, H. Kampwerth, P. Gundel, M.C. Schubert, R.A. Bardos, H. Fill, H. Nagel, P. Würfel, T. Trupke, O. Breitenstein, M. Hermle, W. Warta, S.W. Glunz, Progress in silicon solar cell characterization with infrared imaging methods, Proceedings of the 23rd European Photovoltaic Solar Energy Conference, in: 2008, pp. 965–973.

[5] P. Škarvada, P. Tománek, L. Grmela, S. Smith, Microscale localization of low light emitting spots in reversed-biased silicon solar cells, Solar Energy Materials and Solar Cells 94 (2010) 2358–2361.

[6] P. Koktavy, M. Raska, P. Sadovsky, O. Krcal Noise diagnostics of solar cells, AIP Conference Proceedings 922(2007)141–144.

[7] P. Tománek, J. Brüstlová, P. Dobis, L. Grmela, Hybrid STM/R-SNOM with novel probe, Ultramicroscopy 71 (1998) 199–203.

[8] S. Smith, R. Dhere, T. Gessert, P. Stradins, T. Wang, K. Ramanathan, R. Noufi, A. Mascarenhas, Submicron optoelectronic properties of solar cell materials, Thin Film Compound Semiconductor Photovoltaics, Proceedings of the Materials Research Society 865 (2005) 27–31.

[9] R.H. Martín, C. Dominguez, I. Antón, S. Askins, G. Sala Optics for solar energy, OSA Techn. Digest (CD), Paper STuA4 (2010).

[10] P. Gundel, W. Kwapil, M.C. Schubert, H. Seifert, W. Warta, Approach to the physical origin of breakdown in silicon solar cells by optical spectroscopy, Journal of Applied Physics 108 (2010) 123703.

[11] R. Newman, Visible light from a silicon p-n junction, Physical Review 100 (1955) 700–703.

[12] M. de la Bardonnie, Dong Jiang, S.E. Kerns, D.V. Kerns Jr., P. Mialhe, J.-P. Charles, A. Hoffman, On the aging of avalanche light emission from silicon junctions, IEEE Transactions on Electronic Devices 46 (1998) 1234–1239.

[13] K. Bothe, K. Ramspeck, D. Hinken, C. Schinke, J. Schmidt, S. Herlufsen, R. Brendel, J. Bauer, J.-M. Wagner, N. Zakharov, O. Breitenstein, Luminescence emission from forward- and reverse-biased multicrystalline silicon solar cells, Journal of Applied Physics 106 (2009) 104510 (8pp.).

[14] M.J. Romero, K. Alberi, I.T. Martin, K.M. Jones, D.L. Young, Y. Yan, C. Teplin, M.M. Al-Jassim, P. Stradins, H.M. Branz, Nanoscale measurements of local junction breakdown in epitaxial film silicon solar cells, Applied Physics Letters 97 (2010) 092107 (3pp.).

[15] R. Macků, P. Koktavý, P. Škarvada, Advanced non-destructive diagnostics of monocrystalline silicon solar cells, WSEAS Transactions on Electronics 4 (2008) 192–197.

[16] O. Breitenstein, J. Bauer, K. Bothe, W. Kwapil, D. Lausch, U. Rau, J. Schmidt, M. Schneemann, M.C. Schubert, J.-M. Wagner, W. Warta, Understanding junction breakdown in multicrystalline solar cells, Journal of Applied Physics 109 (2011) 071101 (10pp.).

[17] M. Schneemann, A. Helbig, T. Kirchartz, R. Carius, U. Rau, Reverse biased electroluminescence spectroscopy of crystalline silicon solar cells with high spatial resolution, Physica Status Solidi (A) 207 (2010) 2597–2600.

[18] J-M. Wagner, J. Bauer, O. Breitenstein Classification of pre-breakdown phenomena in multicrystalline silicon solar cells, in: 24th EUPVSEC, 2009, Hamburg, Germany, pp. 925–929.